Light Metals 2011 *Edited by: Stephen J. Lindsay*
TMS (The Minerals, Metals & Materials Society), 2011

CFD MODELLING OF ALUMINA MIXING IN ALUMINIUM REDUCTION CELLS

Yuqing Feng, Mark A. Cooksey, M. Philip Schwarz
CSIRO, Box 312, Clayton South, VIC 3169, AUSTRALIA

Keywords: computational fluid dynamics, aluminium reduction cell, alumina mixing

Abstract

Aluminium reduction cells have been continuously improved to reduce energy consumption and increase metal production rates. One method of reducing energy consumption is to operate the cell at low anode-cathode distances (ACDs). Line currents have been increased to increase production rates, which often requires larger anodes to maintain an acceptable current density. These changes may have a significant impact on aspects of cell performance such as bath flow and alumina mixing.

In previous work, a computational fluid dynamics (CFD) model of bath hydrodynamics and alumina mixing in an aluminium reduction cell has been developed. The bath hydrodynamics has been validated using water model data. In the present work, the CFD model has been used to study the effect of alumina feeder location and feeding strategy in a typical full-scale industrial cell.

Introduction

Bath flow in aluminium reduction cells is important for several reasons. In particular, it dictates the distribution of chemistry and temperature within the cell. Control of alumina dissolution and distribution is important for conventional cells. It has been calculated that a 1 wt% increase in the alumina concentration can increase the metal height (and decrease the bath height) by ~5 mm, i.e. the ACD is reduced by ~5 mm [1]. Significant amperage increases often require a reduction in ACD and/or an increase in anode size, which reduces the amount of bath available to dissolve and distribute the alumina. Furthermore, better alumina control is possibly critical for the implementation of advanced cell designs. For example, it is likely that a cell using inert anodes will require tighter control of alumina concentration to prevent corrosion of the anode [2].

Bath flow can be driven by several mechanisms [3]:

- Release of gas from beneath the anodes;
- Interaction of the magnetic and electric fields in the bath;
- Drag from magnetically induced movement of the metal pad;
- Thermal convection.

It is difficult to directly measure the effect of cell and anode design on bubble-driven bath flow, because of the corrosive nature of cryolite at ~960 °C. Thus when considering an amperage increase, there is often no alternative to trialing the new operational parameters in a number of cells, which is time-consuming and costly. Also, the opposite problem can occur: potential gains from a reduction in ACD and/or an increase in anode size are missed because a multi-cell trial is deemed too time-consuming and costly. Thus there is value in being able to effectively predict the spatial and temporal variation in alumina concentration in an aluminium reduction cell.

In previous work by these authors [4 and references therein], the bath flow and alumina mixing in aluminium reduction cells has been studied using physical modelling and computational fluid dynamics (CFD) modelling of part cell and whole cell geometries. A finding of the previous work was that, for the simple geometry considered, the lowest alumina concentrations are often found in the centre channel. Experimental work by Moxnes et al. [1] using large AlF_3 additions in an industrial cell also suggests spatial variation in the cell. As a result, the alumina feed rate was increased at the two end feeders and decreased in the three central feeders to produce a more even alumina concentration, which suggests that the original situation was lower alumina concentrations at the ends of the cell. These modelling and experimental results suggested that it was worthwhile to investigate the spatial distribution of alumina concentration in the cell in more detail, including modelling the effect of modifying the relative feed rates from different feeders. This is complex, as Moxnes et al. were unable to reproduce the measured flow patterns.

Model Description

Bath flow in an aluminium reduction cell is a typical multiphase flow process, involving strong interaction between gas bubbles and liquid bath due to buoyancy effects, and between liquid bath and liquid metal due to strong electro-magnetic forces. Two types of CFD models have been developed at CSIRO to study bubble driven flow in the bath phase: a small-scale resolved bubble model and a macro-scale time-averaged cell model. The former approach tracks the interfaces around each of the bubbles using, for example, the Volume-of-Fluid (VOF) method, and detailed transient bubbling behaviour can be obtained. However, this model requires a very fine mesh that presents a major hurdle for current computing power. The time-averaged model represents the flow field averaged over time and hence steady state equations are solved. The model also averages over small-scale phase structure (i.e. bubbles) using the so-called two-fluid or Eulerian-Eulerian approach, where gas and liquid are described as interpenetrating continua and equations for conservation of mass and momentum are solved separately for each phase. The model requires less computing power, but the detailed bubbling hydrodynamics cannot be obtained. The former model is suitable for fundamental studies, the latter for process simulation, and has been widely used in various multiphase flow systems, e.g. gas stirred baths [5, 6].

The time-averaged two-fluid modelling approach has been adopted for this study. The governing equations are Navier-Stokes equations in the form for multi-phase flow systems, facilitated with extra source terms to account for the inter-phase actions (e.g. the bubble drag force, bubble induced turbulence). The details of the modelling approach and validation using PIV measurement can be found elsewhere [7, 8].

Model Parameters

There have been very few published CFD studies of alumina mixing in an entire aluminium reduction cell because of the large amount of computer time required. However, to gain a realistic understanding of phenomena such as alumina mixing, it is important to simulate the whole cell. A full-scale cell with 18 anodes was chosen for this study: the geometry represents a typical pre-bake smelter, but is not related to any specific cell design. Figure 1 shows a plan view of the cell geometry. There are four alumina feeding positions, which are modeled in two different arrangements:

1. Roughly equally spaced in the centre channel and in line with the mid-point of anodes ('mid-anode feeders')
2. Located at inter-anode gaps ('inter-anode feeders')

The ACD is 40 mm, the bath depth is 200 mm and the gas flow rate is set to be equivalent to a current density of 0.9 A/cm^2.

A commercial CFD code (ANSYS-CFX12) [9] was used to obtain a numerical solution, where user-defined subroutines have been applied to account for the bubble induced dispersion force and turbulence.

The alumina concentration is set to be 3.5 wt% throughout the cell at the start of the simulation. The alumina feeding strategy is:

1. 22 minutes of underfeeding (1 feed at beginning)
2. 7 minutes of overfeeding (5 feeds 90 s apart)
3. 20 minutes of normal feeding (4 feeds 5 min apart)

Alumina is added as a source term in a region of 200 mm x 200 mm x 20 mm high, with the top of the region being at the bath surface. The standard dump weight for each feeder is 1.65 kg. The model assumes that the alumina dissolves instantaneously.

In this simulation the lowest alumina concentrations are found in the centre of the cell; therefore modified feed rates to produce a more even alumina concentration need to be higher in the centre of the cell and lower at the ends. In the experimental work of Moxnes et al. [1], the feed rates were adjusted significantly; up to 50% at one feeder. For this reason, two additional feed rates are modelled; ±10% and ±30%. A summary of the three feed rates is shown in Table 1. Since there are two feeder locations modeled, this gives a total of six simulations.

Table 1: Alumina feed rates

Feed Strategy	Dump weight (kg)	
	Two centre feeders	Two end feeders
Standard	1.65	1.65
±10%	1.82	1.48
±30%	2.14	1.16

It is important to note the following simplifications in comparison to an industrial cell:

- The anode base is flat and the anode edges/corners are square. This represents a new anode (without chamfers) but most anodes in a cell at any one time have a more rounded bottom profile;
- The side channel and end channel profiles are square and there is no ledge;
- The metal layer is not simulated in the model.

These effects can be important if considering the absolute liquid flows. As this study is comparative (i.e. examining the effect of feeder location and feed rate), the importance of the above effects is reduced.

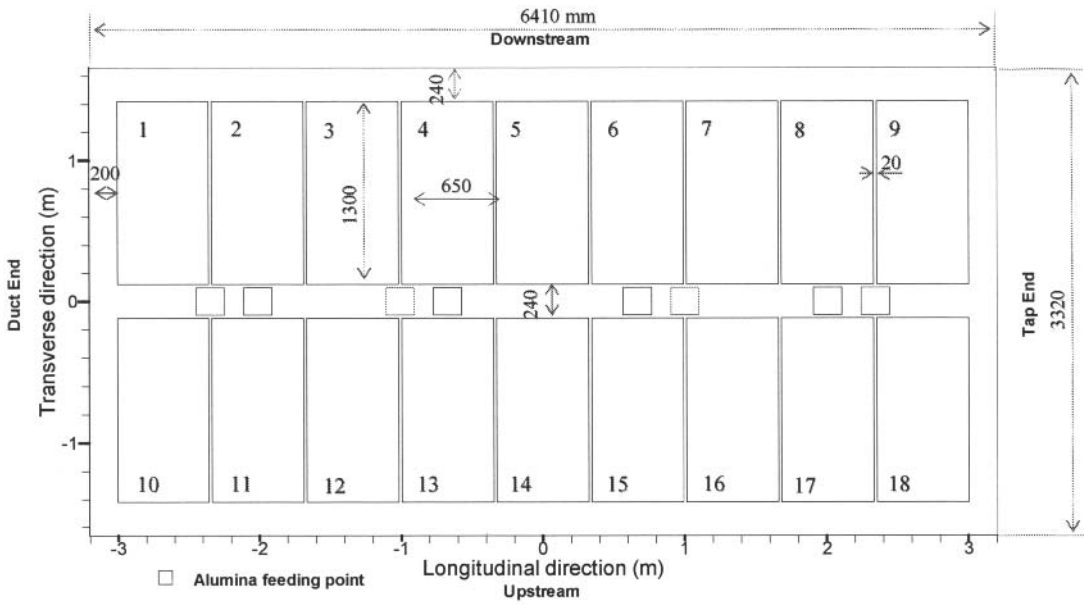

Figure 1: Geometry for full scale CFD model of an aluminium reduction cell; mid-anode feeders shown in black, inter-anode gap feeders shown in red.

Results

The average alumina concentration in the ACD under each pair of anodes through a feeding cycle, for each case, is shown in Figure 3. Only five pairs of anodes are shown because the cell is symmetrical. The data is at one minute intervals.

In all cases, the range of alumina concentrations is low during underfeeding, increases rapidly during overfeeding, and gradually converges during normal feeding. The pattern over multiple cycles was investigated in the CFD model, and it was found that the concentrations tended to converge at the end of overfeeding in each cycle, so the results presented here can be considered representative of repeating alumina feeding cycles.

The range of alumina feeding concentrations (the difference between the highest pair and lowest pair of anodes) at each one minute interval for each case is shown in Figure 4. Overall the range is greater for the inter-anode feeders than for the mid-anode feeders. For the inter-anode feeders, the maximum range is 1.0 wt% alumina for the standard feeding. This range decreases for the ±10% and ±30% feeding; down to 0.7 wt%. For the mid-anode feeders, a different trend is that the range is greatest for ±30% feeding.

From Figure 3, it appears that the minimum and maximum alumina concentrations are generally under the centre and end anodes respectively. A notable exception is the mid-anode ±30% feeding case, where the highest concentrations are under the 6/15 pair of anodes.

As stated, the largest range of alumina concentrations tends to occur at the end of overfeeding; at approximately 30 min. Contour maps of the alumina concentration in the horizontal mid-plane of the ACD at this time are shown in Figure 5. These contour maps show that the spatial variation in the cell is even greater than is apparent from the numerical results discussed to date. There is not just variation from the central anodes to the end anodes, but also from the centre channel to the side channels.

It is striking that the lowest alumina concentrations are found towards the side channels for the central anodes. It appears that the alumina concentration can be 1 wt% higher under the inner half of the anode (towards the centre channel) compared to the outer half.

Increasing the relative feeding rate in the two central feeders does little to increase the alumina concentration in this region. All it seems to do is increase the concentration in the centre channel.

Discussion

The results illustrate the importance of the bath flow in the cell. Note that the bath flow is same for the six cases considered here; it is only the alumina feeding locations and feeding rates that are being modified. The bath flow has been reported previously [10], and the bath velocity vectors for this case are shown in Figure 6.

In previous work [4] it was described that, between feeds, the centre, side and end channels serve as reservoirs of alumina as it is consumed in the ACD, and also that because the centre channel is effectively feeding more anodes than the side or end channels, the alumina in the centre channel can be depleted faster than in the side channel. The present results show that increasing the feed rate of the central feeders addresses the depletion of alumina in the central channel, but has little effect on the side channel.

This can be explained by the fact that the ACD is only 40 mm and the inter-anode gap is only 20 mm, so bath tends to preferentially flow through the centre channel (240 mm) and end channels (200 mm) to the side channel.

The contour maps highlight that feeder location is extremely important. In both cases considered here (mid-anode feeders and inter-anode feeders), it appears that the feeders are too close to the ends of the cell. Significant changes to the relative feeding rates are unable to overcome the effect of feeder location.

The results suggest that there are two broad types of spatial variation in alumina concentration in the cell:

1. Variation along the length of the cell, which can be influenced by feeder location and the relative feeding rates of different feeders;
2. Variation from the centre channel to the side channel, which can be influenced by the ACD and inter-anode gap, and presumably anode slots.

The alumina concentration changes quite quickly in the centre channel and end channel following a feed, but it is slower to change in the ACD and side channels. This gives a guide to the relative speed of alumina processes in the cell, as shown in Figure 2.

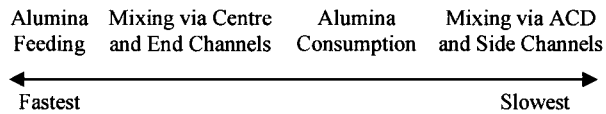

Figure 2: Relative speed of alumina processes in cell.

The results shown that the alumina concentration can vary by 1 wt% due to both types of spatial variation. Given that, as stated previously, a 1 wt% change in alumina concentration can affect the ACD by ~5 mm, the effect of this variation on cell performance may be significant.

Limitations

The model assumes that alumina dissolves instantaneously, which is almost certainly a significant simplification, since sludging of cells is a known problem. Water modelling work by Walker et al. [11] found that the use of crushed ice was superior to a dye tracer in modelling the behavior of alumina in an industrial cell, probably because the crushed ice forms 'rafts' on the liquid surface, as does alumina on the bath surface.

The possible risk of sludging would have to be considered when considering increasing feeding rates at some feeders.

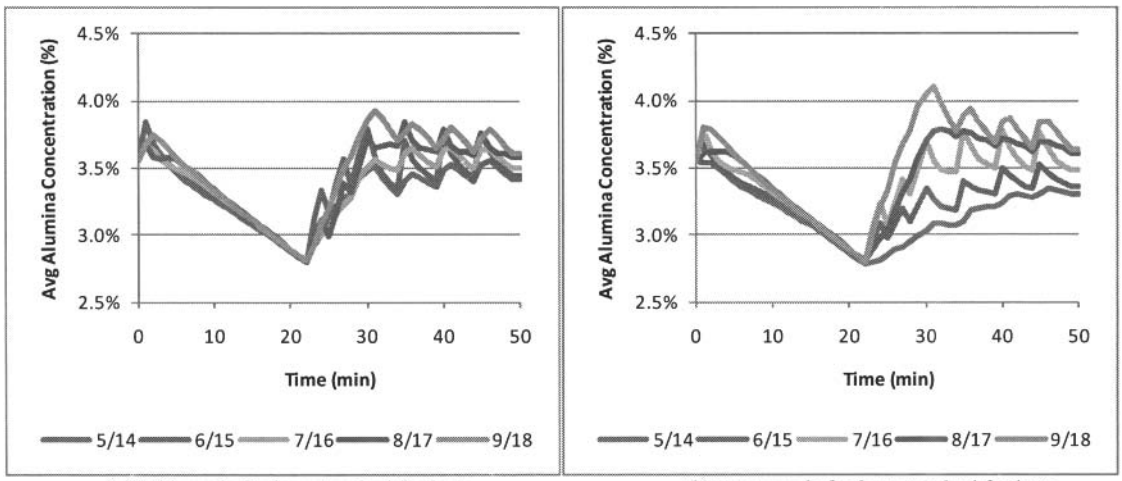

(a) Mid-anode feeders: standard feed rate

(b) Inter-anode feeders: standard feed rate

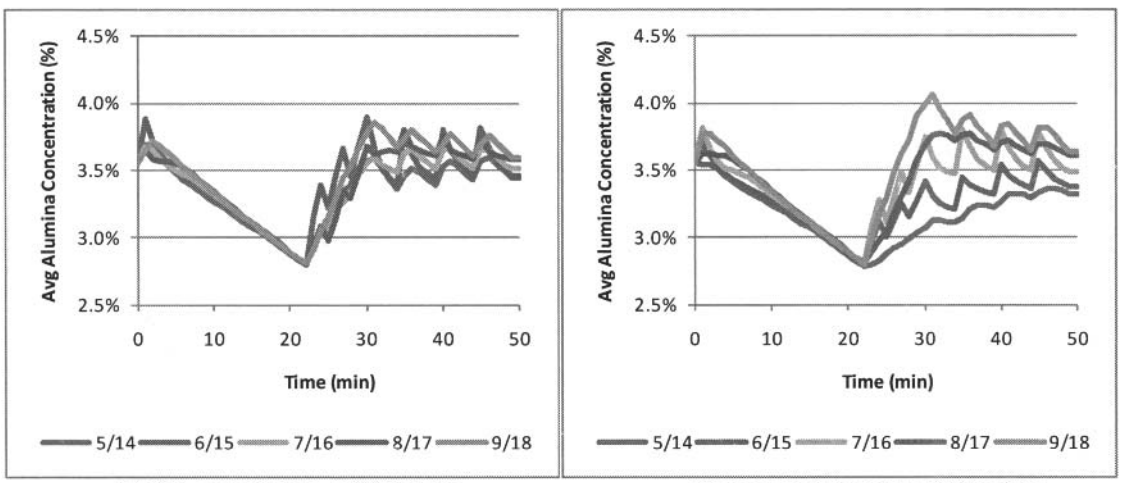

(c) Mid-anode feeders: ±10% feed rate

(d) Inter-anode feeders: ±10% feed rate

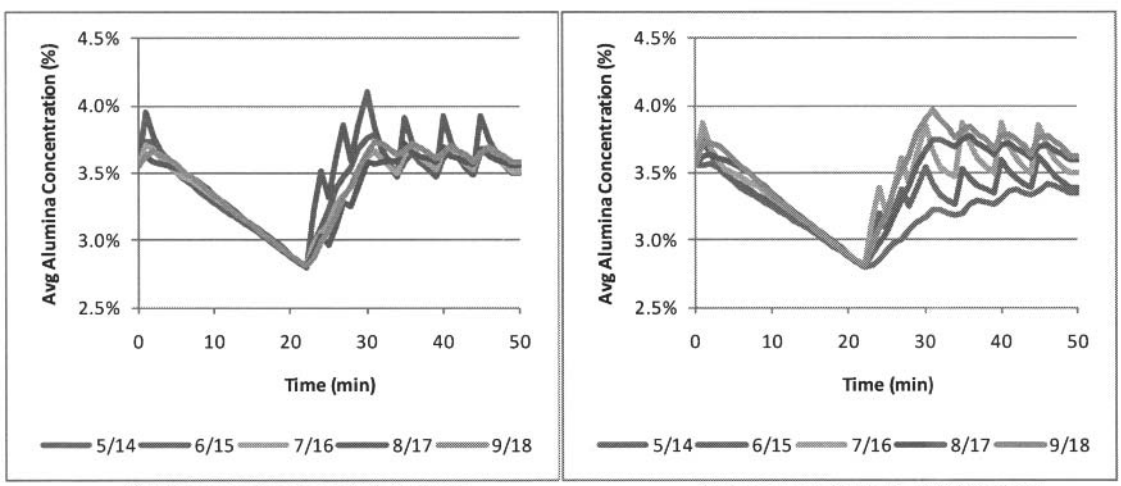

(e) Mid-anode feeders: ±30% feed rate

(f) Inter-anode feeders: ±30% feed rate

Figure 3: Average alumina concentration in ACD under each pair of anodes. Anode numbers in legend are from Figure 1.

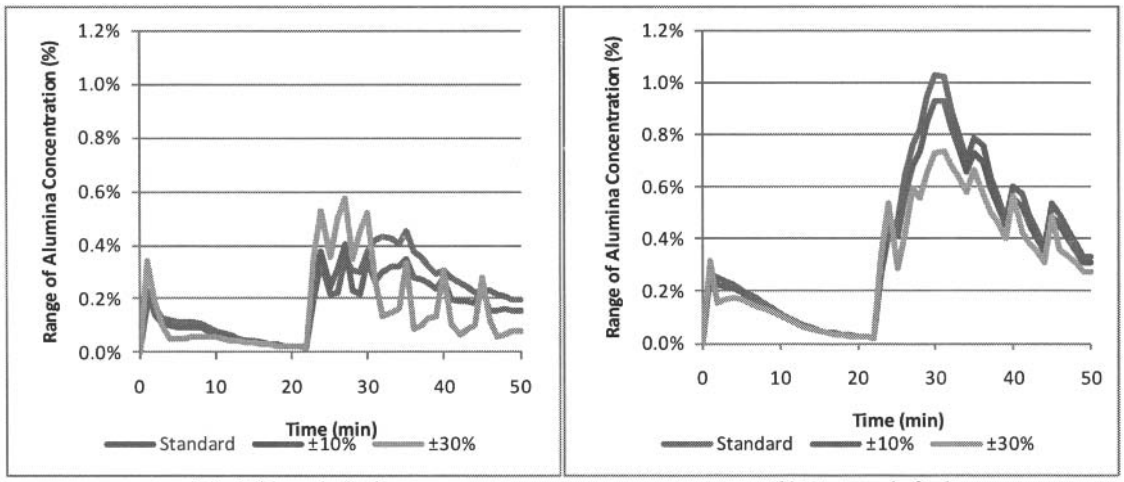

(a) Mid-anode feeders (b) Inter-anode feeders

Figure 4: Range of average alumina concentration under pairs of anodes.

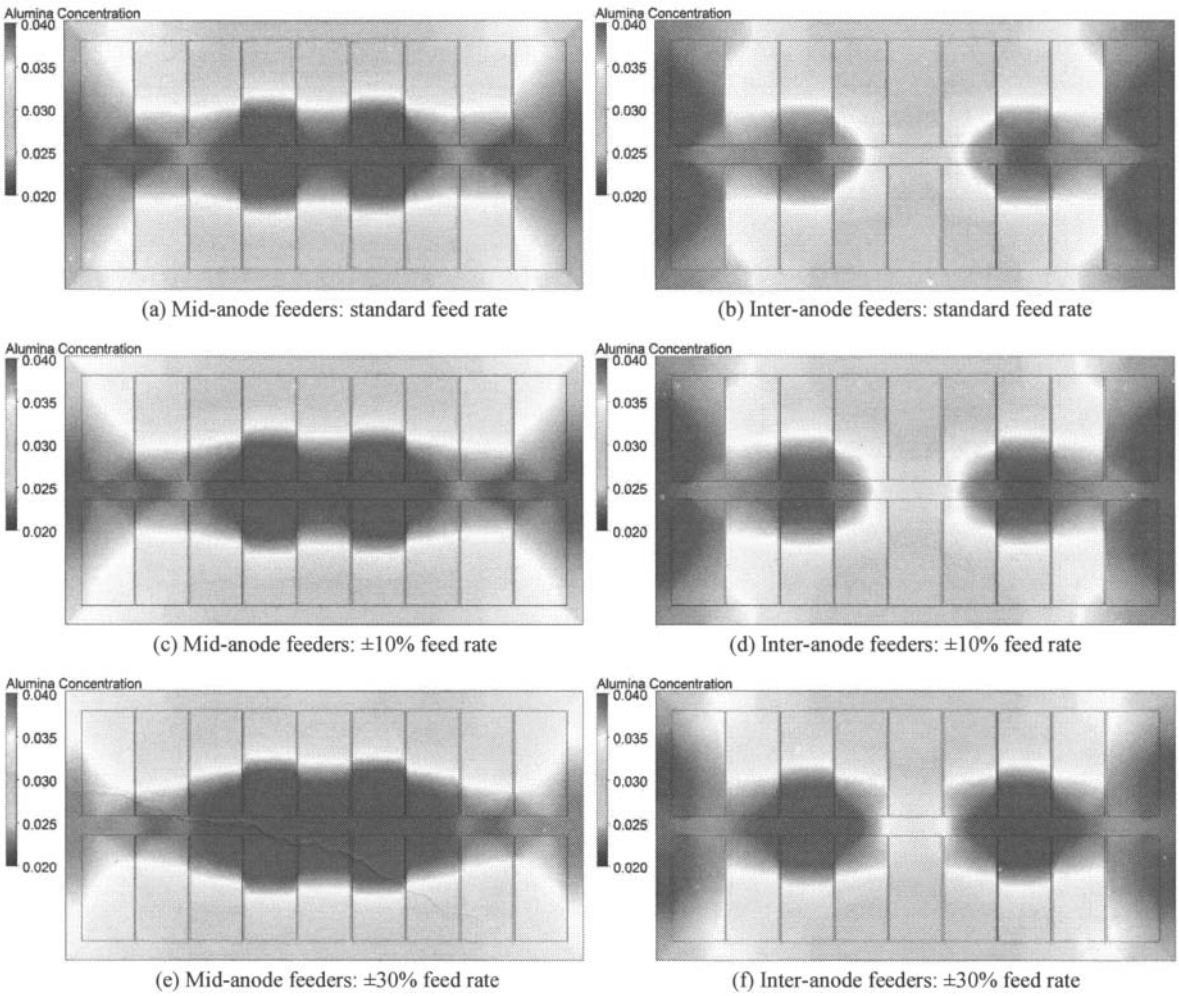

(a) Mid-anode feeders: standard feed rate

(b) Inter-anode feeders: standard feed rate

(c) Mid-anode feeders: ±10% feed rate

(d) Inter-anode feeders: ±10% feed rate

(e) Mid-anode feeders: ±30% feed rate

(f) Inter-anode feeders: ±30% feed rate

Figure 5: Contour maps of alumina concentration in horizontal mid-plane of ACD at around end of overfeeding (30 min).

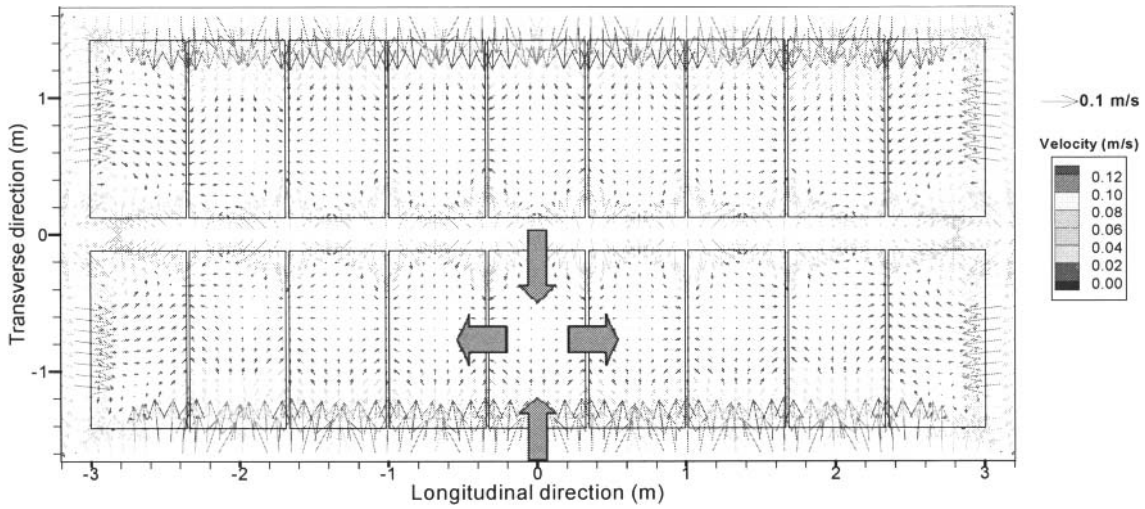

Figure 6: Bath velocity vectors in horizontal mid-plane of ACD (40 mm ACD, 240 mm side channel width) [10].

Conclusions

A time-averaged bubble driven CFD model, validated using water model data, has been extended to study bath flow and alumina mixing in a full scale aluminium reduction cell. The main findings of this study are:

- There can be ~ 1 wt% spatial variation in the alumina concentration, both along the length of the cell and from the centre channel to the side channels.
- Varying the relative feeding rates between different feeders can influence the variation in alumina concentration along the length of the cell. However, this has little influence on the variation between the centre channel and side channels, because this is primarily controlled by the ACD and inter-anode gaps.

These findings demonstrate the effectiveness of CFD modelling for studying the likely effect of various design parameters (e.g. alumina feeder location and feeding rate) on cell performance (e.g. bath flow and alumina mixing). However, the specific results of this modelling should not be over-interpreted, as many of the results are specific to the geometry being considered.

References

[1] B. Moxnes et al., Improved Cell Operation by Redistribution of the Alumina Feeding, *Light Metals 2009*, San Francisco, CA, 15-19 Feb, 2009, 461-466.

[2] J. Thonstad, & E. Olsen, Cell operation and metal purity challenges for the use of inert anodes, *JOM*, *53*(5), 2001, 36-38.

[3] K. Grjotheim, & B. Welch, *Aluminium smelter technology, 2nd edn* (Dusseldorf, Germany: Aluminium-Verlag, 1988).

[4] Y. Feng, M.A. Cooksey and M.P. Schwarz, CFD Modelling of Alumina Mixing in Aluminium Reduction Cells, *Light Metals 2010*, Seattle, WA, 14-18 Feb, 2010, 455-460.

[5] M.P. Schwarz, & W.J. Turner, Applicability of the standard k-ε turbulence model to gas-stirred baths, *Applied Mathematical Modelling*, *12*(3), 1988, 273-279.

[6] G.L. Lane, M.P. Schwarz, & G.M. Evans, Numerical modelling of gas-liquid flow in stirred tanks, *Chemical Engineering Science*, *60*(8-9), 2005, 2203-2214.

[7] Y.Q. Feng, W. Yang, M. Cooksey, & M.P. Schwarz, CFD model of bubble driven flow in aluminium reduction cells and validation using PIV measurement, *Fifth International Conference on Computational Fluid Dynamics in the Process Industries*, Melbourne, Australia, 2006.

[8] Y.Q. Feng, M. Cooksey, & M.P. Schwarz, CFD modelling of electrolyte flow in aluminium reduction cells, *Light Metals 2007*, Orlando, FL, 2007, 339-344.

[9] ANSYS INC CFX12: 2009

[10] Y. Feng, Y., M.A. Cooksey & P. Schwarz, Development of Whole Cell Model of Bath Flow and Alumina Mixing, 9th Australasian Aluminium Smelting Technology Conference, 2007, 14pp.

[11] M.L. Walker et al., Design Considerations for Selecting the Number of Point Feeders in Modern Reduction Cells, *Light Metals 1995*, Las Vegas, NV, 12-16 Feb, 1995, 363-370.